



# Synthesis of graphene oxide at variable pH and its response to antibacterial activity

VARSHA S. HONMORE <sup>A</sup>, AND ASHWINI P. ALEGAONKAR <sup>B,\*</sup>

<sup>a</sup>Post Graduate and Research Center, Department of Chemistry, MES Abasaheb Garware College, Pune-411004, MS, India

<sup>b</sup>Department of Chemistry, Sir Parshurambhau College, Pune 411 030, MS, India

## Abstract

Graphene oxide (GO) is recognized as a potential candidate for the biomedical applications. We report, preparation and use of GO to test its response against Escherichia coli (E-coli), and Staphylococcus aureus (S-aureus) bacteria. Initially, GO is synthesized by modified Hummer's technique, reprecipitated at different pH (@7,10,12, 14) and tested for its antibacterial response, using the diffusion methodology. The HRTEM images shows for GO@7, is extremely transparent showing maximum exfoliation of the conjugated graphitic layers and same is reflected in Raman and intensity of 2D band is remarkably prominent. Notably, GO pH@7 showed maximum efficacy thereby inhibiting more gram-negative bacteria with compared to gram positive. GO pH@7. Further, tests using phosphate buffer that showed total inactivity towards both the bacterial strains. By adjusting pH, externally, GO showed antibacterial activity more than internally adjusted pH for GO. The calculated MIC value for this is 200 µg/mL external buffer.

**Key words:** Graphene oxide, pH, antibacterial activity, zone of inhibition, biomedical applications

<sup>†</sup>Ashwini P. Alegaonkar , Department of Chemistry, Sir Parshurambhau College, Pune 411 030, MS, India

## 1. Introduction

Graphene oxide (GO) is a derivative of graphite, prepared by the oxidation process of graphite. GO layers consisted of oxygen containing functional groups such as epoxide, carboxyl, and hydroxyl groups. These groups are either on the basal plane or present at the very edge of the obtained layers<sup>1</sup>. Due to the presence of oxygen containing groups, GO shows hydrophilic characteristics in nature and is partially soluble in the aqueous medium. Although, traditionally, seen as a precursor to the large-scale synthesis of graphene material, GO has received considerable amount of attention for its possible applications in many numbers of field ranging from bio-medial to mechanical, aerospace to electronics and chemical engineering to catalytic architecting. Moreover, GO is reported to be a useful compound for incorporating in polymer, ceramic, and metal, to form composite with reinforced properties. It is used as a novel form of thin film in electronic writing/printing technologies, hydrogen storage compositions, and for enhanced oil recovery, etc. GO is reported to be antibacterial activity material, due to the edges of graphene layers with extremely high aspect ratio, GO can be used as an ideal nanostructure for an effective destruction of the micro-organisms. Due to its bio-compatibility to human body, it has a potential chemotherapeutic delivery vehicle, envisaged as antibiotic vehicle, with environment compatibility<sup>2</sup>. Moreover there are reports, on GO suspension are biocompatible that can inhibitive for the growth of E-coli with a minimal cytotoxicity<sup>3</sup>, Yuan Chen et al studied and compared the antibacterial activity of four types of GO-based materials such as graphite, graphite oxide, GO, and reduced GO toward a bacteria and model them<sup>4</sup>. His studies concluded that, the antimicrobial actions are contributed by both the membrane and the oxidation stress. Recently, Azad et al synthesized and characterize GO and demonstrated that GO is an effective bactericidal agent against the different superbugs and can be used as a future antibacterial agent<sup>5</sup> in near future. Arshad et al prepared GO–silver nanocomposite and revealed that, the functional groups of GO facilitated the binding of Ag nanoparticles to the GO network that enhanced the antibacterial activity of the nanocomposite. Further, GO was functionalized with the cellulose acetate membrane<sup>6</sup>, copper<sup>7</sup>, and rose bengal/polyvinyl alcohol hybrid hydrogel (RB/PVA/HD)<sup>8</sup> to investigate antimicrobial activity. In a study, a GO-nanocomposite was prepared using the triarylmethane based antibacterial ionic liquid<sup>9</sup>. Multifunctional graphene hybrid film was fabricated by incorporation of the antibacterial protamine<sup>10</sup>. GO/nickel oxide nanocomposite<sup>11</sup>, zeolite/silver/GO nanocomposite were prepared with a high-performance antimicrobial activity with a suitable cytocompatibility<sup>12</sup>. Among the reported techniques, GO

synthesized with at a different value of pH has not been examined. Variable pH has advantage over a fixed value. In the current communication, we have synthesized GO at different pH and examined for its antibacterial activity against E. coli and S-aureus.

## 2. Experimental

### 2.1 Preparation of GO and rGO

GO is synthesized from the readily available graphite by using modified Hummer's technique<sup>13</sup>. GO at different pH was prepared by varying the pH of the solution using 10% sodium hydroxide (NaOH). Initially, 10% NaOH solution was added till the desired pH was achieved under vigorous continuous stirring. Further, precipitated of GO was separated by the centrifugation methodology and obtained material was washed for several times with the double distilled water. The pH was measured using pH meter at 300K.

### 2.2 Material characterizations

FTIR measurements were performed over 400-4000  $\text{cm}^{-1}$  (Make/Model: Bruker Tensor 37). Raman measurements were performed over 200-3500  $\text{cm}^{-1}$  (Make/Model: using LABRAM HR800) with photo-excitations @632 nm. XRD measurements were carried out using Cu  $K\alpha$  radiation@ $1.5406\text{\AA}$  (Make/Model: Brukar 7739) with  $2\theta$  over the range of 10-90° and scan speed  $2^\circ\text{m}^{-1}$ . FESEM imaging was carried out on GO and bacteria treated GO at 20 kV beam potential with 5.5 mm working distance and at different magnifications (Make/Model: Zeiss 7090). HRTEM imaging of GO@pH was carried out at 500 kV beam potential at different magnifications (Make/Model: Jeol, 7609).

### 3. Results and discussion

#### 3.1 Analysis of GO@pH solution

Figure 1 (a) shows FTIR spectra for 7-14 pH values. A band around  $3430\text{ cm}^{-1}$  has been observed, typically, for pH 7 and 10 solution which corresponds to the -OH str. band. Similarly, peaks emerged  $\sim 1000$  are assigned for the epoxide moiety,  $\sim 1600$  for C=C. They are seen for all the samples which supported the fact that the proper oxidation of graphite has been taken place. The peak appeared at  $\sim 1740\text{ cm}^{-1}$  is attributed to C=O, and bands between 1600-1640 are assigned for the aromatic C = C bond (str. vibrations),  $\sim 873$  for =C-H bend. vibrations.

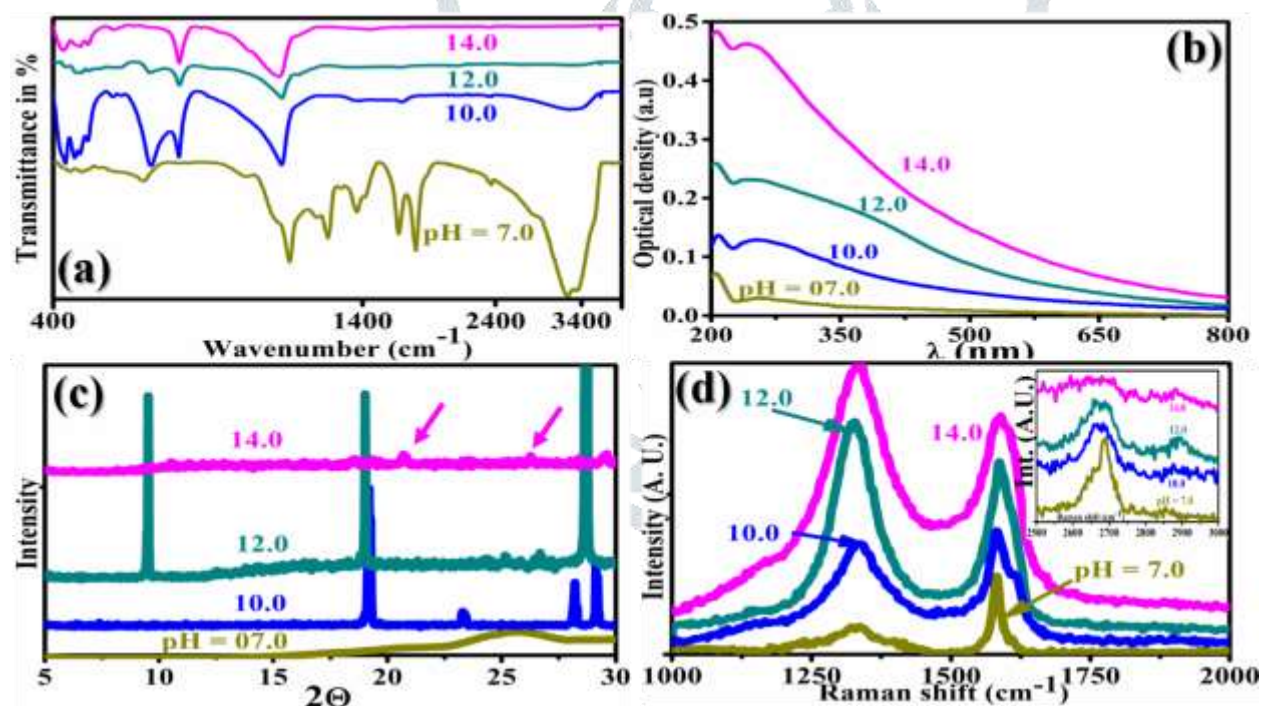


**Figure 1:** Recorded (a) FTIR, (b) UV-vis, (c) XRD, and (d) Raman data for pH 7, 10, 12, and 14 GO solution.

The infrared data is in good agreement with the reported literature<sup>14</sup>. The presence of oxygen related functional groups are noted for not all samples which may be due to the different extent of oxygen content in different pH solutions. Particularly, @pH 7, bands are appeared to be sharp, prominent, however,

broader when compared with other pH solutions. This is attributed to the high percentage of functional -OH group present in the solution.

Figure 1 (b) shows recorded UV-vis spectra for GO @different pH. For these samples, the UV peaks are noted at wavelength position of ~ 250, 280, 317, and 347 nm. Clearly, it is due to the presence of various functional groups present therein and are attributed to the transition between  $n$  to  $\pi^*$  and  $\pi$  to  $\pi^*$  electronic energy levels<sup>15</sup>. With increases pH and GO precipitation, the peaks are observed to be red shifted marginally. This is due to the increase in conjugation by the existence of the functional groups on the graphene layers. Hence, we took GO which synthesized at pH 7 for further studies.

Further, Figure 1(c) shows the typical powder diffraction patterns recorded for of GO@7,10, 12, and 14 pH values. A significant variation in the nature of diffraction pattern has been seen for variable GO@pH. For pH@12 a characteristic GO peak is appeared at  $\sim 10^\circ$ , whereas, the other two peaks recorded at  $19^\circ$  and  $28^\circ$  are the graphitic phases present in the samples. For GO@14, the peaks are observed to be suppressed dramatically and it seems that the total crystallinity of the sample is lost, whereas, for GO@7 all the other peaks are absent except a broad peak emerged at  $\sim 25^\circ$  which is attributed to the graphene-like crystalline flakes. Using Bragg's equation, interplanar distance is calculate. The value of interplanar distance for GO@12 and 10 is  $\sim 2.02 \text{ \AA}$  and for GO@7  $\sim 4.67 \text{ \AA}$ . This is an indicative of the unprecedented increase in the interlayer distance at pH 7. Moreover, such pH could be more effective in preparation of the graphitic intercalation compound. Notably, all calculated d-values are in order with JCPDS 75-2078 card.

Raman is a sensitive technique to characterize carbon compounds, particularly, composition and attachment of the functional group to graphitic layers. Figure 1(d) shows recorded Raman spectra at 632 nm excitation for various GO@pH. Table 1 shows position of D, G, 2D bands for corresponding GO@pH.

**Table 1:** Position of D, G and 2D for variable pH GO solution.

GO @pH	G ( $\text{cm}^{-1}$ )	D ( $\text{cm}^{-1}$ )	2D ( $\text{cm}^{-1}$ )
7	1580	1338	2673
10	1584	1340	2670
12	1593	1351	2674
14	1592	1357	-

Recorded Raman peaks are quite distinct which shows variations in bond molecular environment with change in pH. For GO@7, the D-peak is recorded to be very broad with a shallow shake up. The presence of such feature is attributed to the rupture of C=C and attachment of polar functional groups resulting transformation of G site to D. Wherein, the G peak is observed to be very sharp and consisted of broadening at higher wavenumber which is due to residual stress between opened up C=C site and attachment of corresponding functional moiety.

For GO@10, identical trend has been seen with a very prominent split of G-peak and the trend continued for 12. The position of D band is almost invariable for all pH values, whereas, position as well as intensity of the 2D band is observed to be varied for the solutions. For pH @14 the 2D band is completely disappeared, whereas, for pH@7 the intensity of 2D band is remarkably prominent. The dramatic variations in 2D are indicative of significant change in layer conjugation. It seems that GO@7 has highest degree of intercalation over others. By and large, the shift in D peak is recorded to be 2% and 15% for G peak with respect to positions recorded for GO. Further, GO@pH are investigated for their degree of exfoliation using HRTEM imaging. Figure 2 shows recorded HRTEM images for GO@pH for 7, 10, 12, and 14. The scale bar is 500 nm.

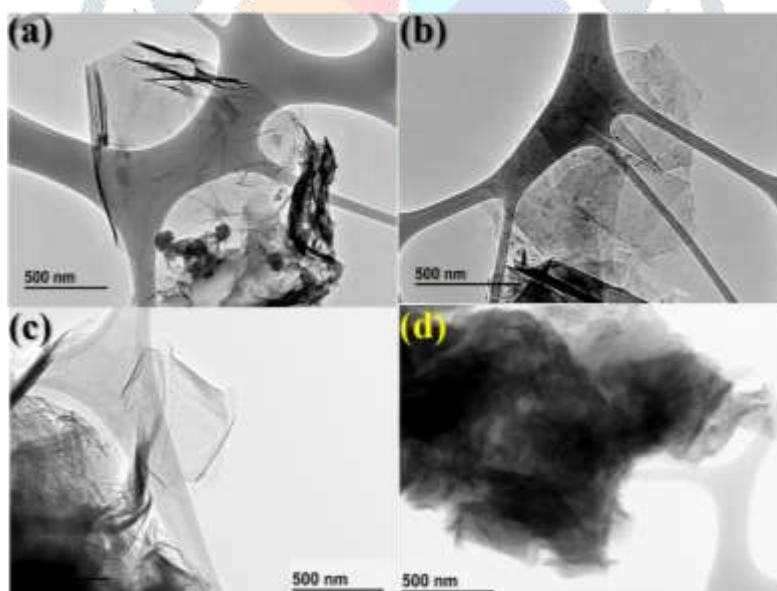


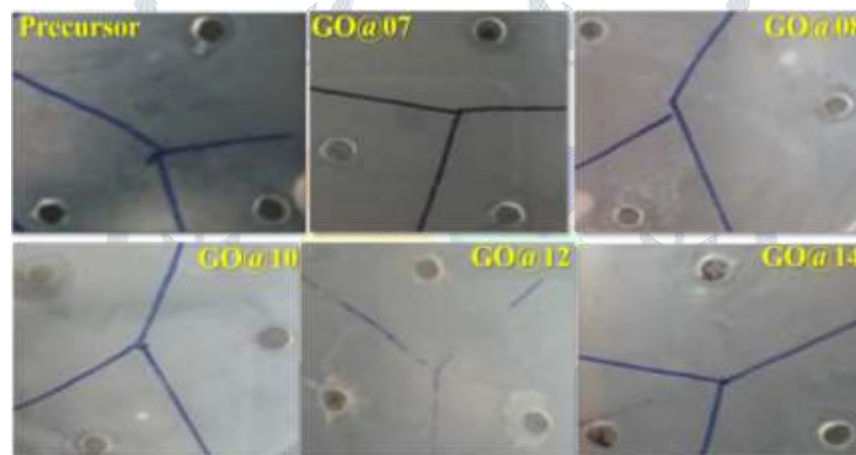
**Figure 2:** Recorded HRTEM images for GO@pH for (a) 7, (b) 10, (c) 12, and (d) 14.

One can see from the recorded images that, for GO@7, i.e. Figure 2(a), is extremely transparent showing maximum exfoliation of the conjugated graphitic layers. Hardly bunch/conjugation of layers are visible in (a). For Figure 2(b), number of layers are seen, overlapping each other. Perhaps some zone (at the bottom) has appeared to be dark

showing inhomogeneous exfoliation for GO@10. Whereas, for GO@12 and 14, i. e., respectively, Figure 2(c) and (d) one can see the conjugated layers are bunched quite prominently showing larger thickness of G flakes.

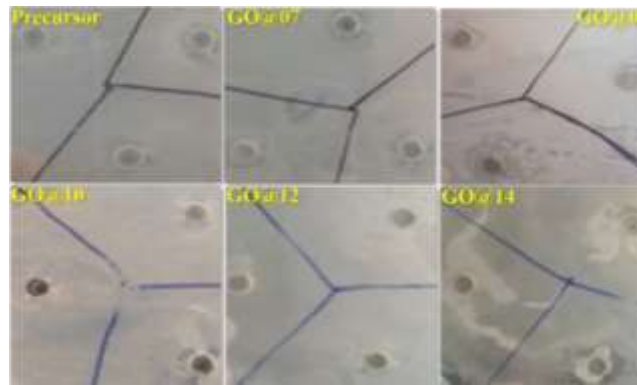
### 3.2 Analysis of antibacterial activity: GO@pH

The antimicrobial activity of the GO@pH is tested against the two types of test organisms first gram negative, E-coli, and, secondly, gram positive, S-aureus using well diffusion method. For this purpose, GO@pH is incubated with bacteria of about 24 h with subsequent imaging of zone of inhibition. Figure 3 shows recorded photographic images for GO@pH for 7,8,10,12, and 14. Typical results are presented in Table 2. Detailed figures are shown in supplementary information Figure(1)



**Figure 3:** Incubation of GO@pH for 24 h with E-coli recorded in photographic images showing zone of inhibition.

In similar fashion, the experiment was conducting using gram positive, S-aureus cell culture. Notably, no zone of inhibition is recorded for S-aureus in contrast to gram negative, E.coli. It is also observed that, GO@7 pH has larger zone of inhibition compared others GO@pH.



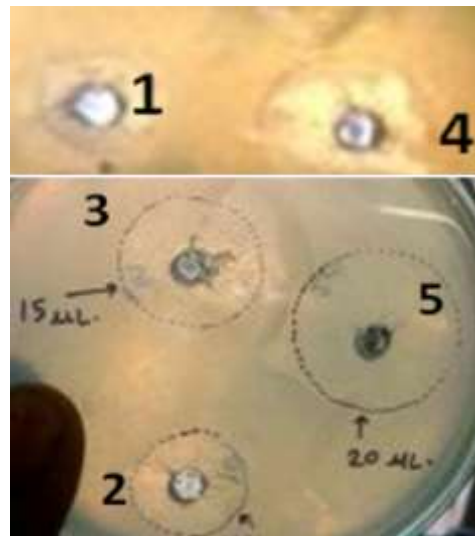
**Figure 4:** Recorded photographic images for GO@pH for 24 h incubation with S-aureus showing no establishment of zone of inhibition.

Figure 4 shows recorded zones of inhibition for GO@pH after 24 h of incubation time for gram positive S-aureus cell culture. It seems that, the GO@pH is in effective for gram positive bacteria over gram negative.

**Table 2:** Response of GO@pH for gram negative (E-coli) and positive (S-aureus) bacteria for incubation period of 24h. The value of 0.0 shows incubation of no zone of inhibition by the bacteria.

GO@pH	Zone of inhibition (in cm)	
	E-coli	S-aureus
7	2.5	0.0
10	0.5	0.0
12	0.6	0.0
14	0.0	0.0

From the analysis, it has been observed that, GO@7 pH comprised of large zone of inhibition over other pH solutions of GO. Moreover, structure-property relationship analyzed by the other characterization techniques showed peculiar morphology of GO@7 pH. Depicting these observations, we had chosen GO@7 pH for further antimicrobial studies. For this purpose, we prepared different concentrations of GO@7 pH in order to examine the minimal inhibitory concentration (MIC) using diffusion method as discussed above. The culture was incubated at 37°C for 24 h. Figure 5 shows recorded zone of inhibition after 24 h of incubation of GO@7 pH for E-coli bacterial colony. Detailed figures are shown in supplementary information Figure(2)



**Figure 5:** Recorded antimicrobial activity for gram negative E-coli at GO@7 pH with variable concentration 05-20  $\mu\text{L}$ .

**Table 3:** Data for zone of inhibition obtained for different concentration of GO@7 pH.

Location	Concentration (in $\mu\text{L}$ )	Zone of inhibition (in cm)
1	05	1.5
2	10	1.9
3	15	2.3
4	20	2.9
5	30	3.2

It has been found that, MIC for GO@7 pH is 5 $\mu\text{L}$  having zone of inhibition 1.5 cm, whereas, concentration lower than 5 $\mu\text{L}$  did not showed formation of proper zone of inhibition. With six-fold increase in concentration, the increase in zone of inhibition is twice.

Further, we attempted to investigate the effect of GO@pH by externally adjusting using a buffer solution such as the phosphate buffer. The details of preparation procedure of buffer solution are provided in the supplementary information and the results are obtained using well diffusion method are shown in Figure 6. Detailed figures are shown in supplementary information Figure (3)

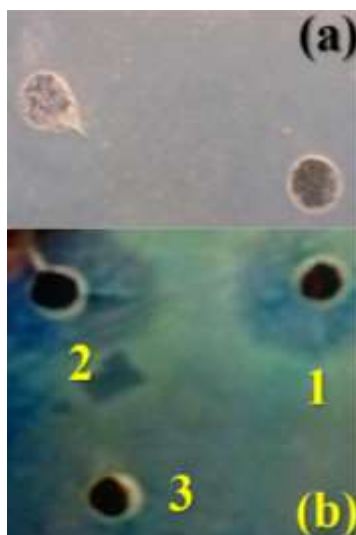


**Figure 6:** Recorded antimicrobial activity for gram negative E-coli at GO@7 pH with externally adjusting pH using phosphate buffer. (a) only phosphate buffer showing no zone of inhibition, and (b) showing site 1@5  $\mu$ L with 2 cm zone, site 2@2  $\mu$ L with 1.5 cm, and site 3@1  $\mu$ L no zone reported.

As seen in Figure in 6(a), by examining the antimicrobial activity of the buffer solution it is concluded that no activity contributes from the buffer, hence, activity is due to the GO. From Figure 6(b), it has been found that, when the phosphate buffer is used externally for adjusting GO@7 pH solution, the overall antimicrobial activity of the GO@pH solution is increased. Moreover, solution with 2  $\mu$ L concentration is seen to be effective to counter the E-coli. The value of MIC is estimated which has been obtained for 200  $\mu$ g/mL external buffer. From Figure 6(b), one can see that, for 1  $\mu$ L no zone of inhibition is seen. In parallel, antibacterial activity of the rGO is also examined by adjusting external pH@7 using phosphate buffer as well as in situ maintaining pH during synthesis. Following table i.e. Table 4 shows the antimicrobial activity. By adjusting pH, externally, GO showed antibacterial activity more than internally adjusted pH for GO.

**Table 4:** Data record for observed zone of inhibition with GO@pH external and internal.

Sr. No.	Concentration@GO@pH 7 (external vs internal)	Zone of inhibition (in cm)
1.	15 $\mu$ L pH@external	1.9
2.	05 $\mu$ L pH@internal	0.0
3.	30 $\mu$ L pH@external	1.7

Further, GO@7pH@external with MIC obtained at 200 µg/mL has been chosen for making the bacterial solution. Preparation of the bacterial solution is carried out using bacterial culture of E-coli cell in 0.9% of NaCl. The preparation details are provided in supplementary information.

Notably, in current investigations, the zones of inhibitions are observed, however, with intermittent presence. The possible reasons are concentration of GO@7 pH introduces well-structured composition which is compatible with the cell wall. Thus, high degree of exfoliation enhances the antimicrobial activity. In general, the action of GO onto the organisms is due to the cell wrapping. The direct contact of the extremely sharp edges of GO with the plasma membrane of cell induces oxidative stress which results into physical damage of cell leading to the loss of membrane integrity and leakage of ribonucleic acid (RNA).

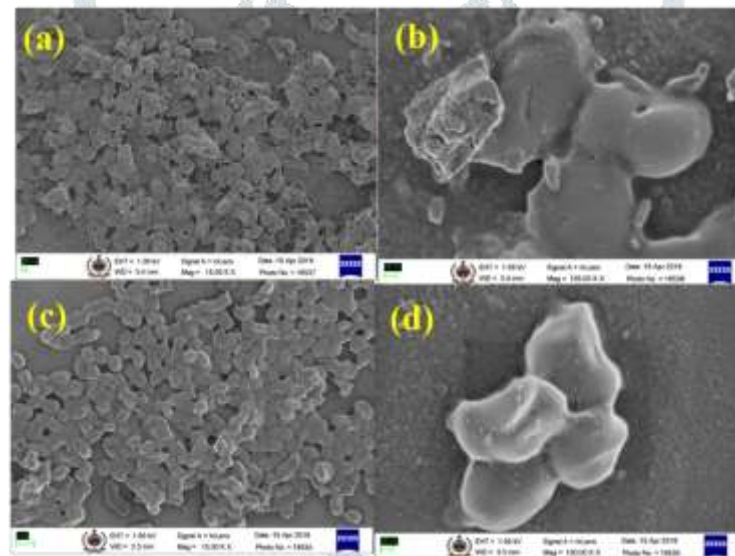


**Figure 7:** Recorded FESEM images for GO@7pH (a) GO @pH 7 after incubation for 24 hrs (b)GO@ external (a) GO @pH 7 after incubation for 24 hrs (b) (c) and (d) control

It seems that, for E-coli, due to the single layered peptidoglycan present, in general, in gram negative organism, in presence of  $sp^2$  hybridized GO with atomically sharpened basal edges are able to penetrate the outer-membrane of the bacteria. As a consequence, the bacteria cell releases the lipid content due to which cells loses their viability resulting antimicrobial activity as seen and discussed in the results. For gram-positive, S-aureus, the peptidoglycan

comes in multilayered format and offer toughness. This made S-aureus resistant to the physical disruption from GO. Moreover, it has been reported that, under the stressful conditions; S-aureus is able to produce the dormant endospores to remain inactive. Due to these reasons, it did not showed significant amount of antimicrobial activity than E-coli.

#### 4. Conclusion

We have successfully graphene oxide from graphite at various pH conditions viz 7, 10,12and 14. The antibacterial activity@ pH 7 against E-coli was very effective. On comparing to internal pH adjustment for sample by using NaOH, externally adjusted pH 7 by using phosphate buffer shows good results with MIC value 200 µg/mL. The IR spectra shows GO -OH C=C, C=O str. Band and =C-H bend. vibrations indicating oxidation of graphite. It may be attributed to pressure or oxidative stress of COOH, OH group, and maximum exfoliation as compared to other samples. The powder XRD GO@7 all the other peaks are absent except a broad peak emerged at  $\sim 25^{\circ}$  which is attributed to the graphene-like crystalline flakes. The Raman spectra shows, the D-peak s recorded to be very broad indicates the presence of such feature is attributed to the rupture of C=C and attachment of polar functional groups resulting transformation of G site to D. The G peak is observed to be very sharp and consisted of broadening at higher wavenumber which is due to residual stress between opened up C=C site and attachment of corresponding functional moiety. The HRTEM illustrates extremely transparent showing maximum exfoliation of the conjugated graphitic layers. The FESEM shows evidence for the bacterial activity. For externally adjusted pH of GO pressure of phosphate anion which are rich in oxygen contain are responsible for antibacterial activity. But for phosphate buffer itself, it has no antibacterial activity. It can be thought that E-coli, due to the single layered peptidoglycan present, in general, in gram negative organism, in presence of  $sp^2$  hybridized GO with atomically sharpened basal edges are able to penetrate the outer-membrane of the bacteria. As a consequence, the bacteria cell releases the lipid content due to which cells loses their viability resulting antimicrobial activity.

**Acknowledgements :** Authors are thankful to Dr. Prashant S.Alegaonkar, Dept of Physics,CUPB, Batinda, Punjab for providing Raman, HETEM, FESEM facilities.

**References:**

1. Y. Hernandez, M. Lotya, V. Nicolosi, F.M. Blighe, S. De, G. Duesberg and J.N. Coleman  
*J. Am. Chem. Soc.*, **131**, 3611(2009).
2. V.C Sanchez, A. Jachak, R. H. Hurt and A. B. Kane, *Chem. Res. Toxicol* ,**25**, 15,2012.
3. I. Sheet, H. Holail, Z. Olama, A. Kabbani and M. Hines, *Int. J. Curr. Microbiol. Appl. Sci*, **2**, 1, (2013).
4. S. Liu, T.H. Zeng, M. Hofmann, E. Burcombe, J. Wei, R. Jiang, J. Kong, and Y. Chen, *ACS nano*, **5**, 6971, (2011).
5. M. T. H. Aunkor, T.Raihan, S.H. Proadhan, H.S.C. Metselaar, S.U.F Malik, and A.K. Azad, *R. Soc. Open Sci.*, **7**, 200640 (2020).
6. M. Zahid, S. Akram, A. Rashid, Z.A. Rehan, T. Javed, R. Shabbir, M.M. Hessien, and M.E. El-Sayed, *Membranes*, **11**, 5102021(2021).
7. X.Song, L. Xie, M. Zhang, W. Wang, L. Li, X. Lu, P. Lei, D. Liu, Y.Chen, H. Chen, C. Zhao. Cu-decorated graphene oxide coatings with enhanced antibacterial activity for surface modification of implant. *Mater. Res. Bull.*,**141**, 111345 (2021).
- [8] S. Prusty, K.Pal, D. Bera, A. Paul, M. Mukherjee, F. Khan, A. Dey, S. Das, S, *Colloids and Surfaces B: Biointerfaces*, **203**, 111729 (2021).
- [10] X. Feng, J. Wang, P. Cai, Z. Yang, J. Shen, Y. Zhang and X. Zhang, *Colloids and Surfaces A: Physicochemical and Engineering Aspects*, **625**, 126977 (2021).
- [11] S. Archana, B.K. Jayanna, A. Ananda, B.M. Shilpa, D. Pandiarajan, H.B. Muralidhara, and K.Y. Kumar, *Environmental Nanotechnology, Monitoring & Management*, **16**, 100486 (2021).
- [12] Abed, S. H.R. Ning, A. Sadeghianmaryan, and X. Chen. Antibacterial activities of zeolite/silver-graphene oxide nanocomposite in bone implants. *Materials Technology*, **36**, 660 (2021).
- [13] Jr Hummers, S. William, and E. Richard Offeman, *J. Am. Chem. Soc.* **80**, 1339 (1958).
- [14] A. P. Alegaonkar, P.S. Alegaonkar, and S.K. Pardeshi, *Mater. Chem. Phys*, **195**, 82(2017).
- [15] A.P.Alegaonkar, K.C. Tripathi, H.B. Baskey, S.K. Pardeshi and P.S. Alegaonkar, *ChemNanoMat*, **7**,1,(2021).